Investigation of the variability of night-time equatorial thermospheric winds over Nigeria, West Africa

[1,3]Rabiu, A. B., [1,3]Okoh, D. I., [2]Wu, Q., [4,5]Bolaji, O. S., [6]Abdulrahim, R. B., [1]Dare-Idowu, O. E., [1]Obafaye, A. A.

[1]Centre for Atmospheric Research, National Space Research and Development Agency, Anyigba, Nigeria

[2]National Center for Atmospheric Research, High Altitude Observatory, Boulder, USA

[3]Institute for Space Science and Engineering, African University of Science and Technology, Abuja, Nigeria

[4]Department of Physics, University of Lagos, Nigeria

[5]Department Mathematics and of Physics, University of Tasmania, Australia

[6]Centre for Satellite Technology Development, National Space Research and Development Agency, Abuja, Nigeria

Correspondence: Rabiu, A. B. (tunderabiu2@gmail.com; +2348030705787) and Okoh, D. I. (okodan2003@gmail.com; +2348136094616)

Abstract

This paper examined the variability of equatorial thermospheric meridional and zonal wind speeds at night-time using an optical Fabry–Perot interferometer (FPI) located in Abuja, Nigeria (Geographic: 8.99°N, 7.39°E; Geomagnetic latitude: -1.60). The study period covered 9 months with useable data of 139 nights between March 2016 and January 2018. The hourly zonal wind speed is between 19.33 and 250 ms^{-1} and that of the meridional wind ranged between 0 and 200

ms^{-1}. These speeds are greater than those reported in other longitudinal sectors, and this could be one of the reasons responsible for reduced EXB drift in this region compared to other regions. Comparison of FPI ground-based measurements with estimates from the Horizontal Wind Model (HWM-14) accurately reproduced the meridional component, but for some departure of ~45 ms^{-1} in May and June 2016, and January 2018. A very good agreement is observed between the predicted and measured zonal winds speed in the months of 2017. However, the HWM-14 overestimated the zonal wind speed in the early evening values by ~30 ms^{-1} and underestimated the post-midnight values by a larger factor in December 2017. Hence, this necessitates a call for improvement of the HWM-14 by using newly observed data in order to better characterize the West African sector. The varying zonal winds showed modal periods of 25.9 and 133.5 days, which are quasi 27-days and quasi-terannual periodic variations, respectively. On the meridional wind, oscillatory periods of 133.5 and 23.1 days are seen in year 2016 and 2017, respectively.

Key words: Thermospheric winds, FPI, meridional, zonal, Doppler shift, periodogram, airglow.

1. Introduction

From the work of Delinger (1939), we began to understand that complex behaviour of ionospheric currents and electric fields during quiet and magnetically active periods are partly affected by thermospheric neutral parameters such as wind velocity, density and temperature. The coupling of these modulated ionospheric currents and electric fields due to some of these thermospheric neutral parameters with the F-region and its top side can degrade navigation systems and attenuate radio signals (Wernik et al., 2004; Yoon et al.,

2014; Panda et al., 2018). In order to give reasonable description of these thermospheric-ionospheric dynamics, and proffer solutions to many of these adverse effects of ionospheric irregularities/scintillations and modulated latitudinal distribution of low latitude plasma after fountain effect on our ground- and space-based assets, two very important thermospheric neutral parameters; neutral wind and temperature from the Fabry–Perot Interferometers (FPI) have being extensively investigated. Such comprehensive details with regards to FPI neutral wind and temperature profiles can be found in the works of Burnside et al. (1981), Killeen et al. (1995), Raghavarao et al. (1998), Wu et al. (2004), Shiokawa et al. (2012) and Yiyi et al. (2012).

In all of these investigations, African varying thermospheric winds have not been observed experimentally until November 1994 to March 1995 (Vila et al., 1998). In this pioneer work over an equatorial West Africa station, Vila et al. (1998) found persistent eastward flow of zonal winds. In regards to the irregular varying northward and southward meridional (higher than 50 ms^{-1}) neutral winds that modulated the near-equatorial F2 peak distributions, they frequently persist northward in the early evening periods. This confirm that experimental observations of neutral wind and temperature in Africa have not been well-documented until 2017 (Tesema et al., 2017) in Bahir Dar, an equatorial station in Ethiopia, East Africa. This was followed by Malki et al. (2018) in Morrocco, a middle latitude station (North Africa). For updates, Tesema et al. (2017) observed maximum equatorward and poleward wind of around 20-50 ms^{-1} and ~ 100 ms^{-1} in the early evening during quiet conditions in equinoctial and winter months, respectively. In the works of Malik et al. (2018) during magnetically active periods, equatorward wind reached 120 ms^{-1} prior to local midnight and the maximum zonal wind stood at 80 ms^{-1} after local midnight.

After Vila et al. (1998) work until now, there is no comprehensive experimental observation of thermospheric neutral wind in West African equatorial station. This unexplored experimental thermospheric neutral wind in equatorial region of West Africa, which have not been filled-up until now have left some scientific questions unanswered. For example, the effect of thermospheric neutral winds coupling ions (Jones et al., 2013; Maute et al., 2015) in addition to the difference in the geomagnetic main field with respect to the dip equator (Rabiu et al., 2011; 2017; Yizengaw et al., 2014; Bolaji et al., 2016) has been suggested as the facilitator of significant discrepancies in the longitudinal distributions of equatorial electrojet (EEJ) strength/inferred EXB drift between Africa and other regions. However, the geomagnetic main field with respect to the dip equator in Africa is almost horizontal. Now, one of the unresolved scientific questions is, what can be responsible for the longitudinal difference in electric fields within equatorial Africa? We understood that statistical analysis of thermospheric neutral wind in equatorial West Africa is very important to unravel possible mechanisms responsible for this longitudinal difference in ionospheric dynamics within Africa equatorial region and around the world.

In order to achieve this statistical analysis, we used FPI data from Abuja (an equatorial station in Nigeria) for a 9-month period (139 observation nights) during quiet conditions between March 2016 and January 2018. The values of these equatorial thermospheric neutral winds are then compared with those of other regions for possible connection with regards to the longitudinal difference that have been reported in ionospheric dynamics along the equatorial region around the world. We also estimated the wind data from the Horizontal Wind Model-14 (HWM14) and verified it against experimental data from the FPI. Periodicities associated with these thermospheric neutral winds are also studied. The

FPI instrument, its dataset, and the data processing technique used in this study are described in section 2. In section 3, we presented the results and discussed them. The conclusions and outlooks are drawn in section 4.

2. Data and Methodology

Thermospheric meridional and zonal wind speeds were obtained at night-time using an optical Fabry–Perot interferometer (FPI) located at the Space Environment Research Laboratory (SERL), Centre for Atmospheric Research (CAR), Abuja, Nigeria (Geographic: 8.99°N, 7.39°E; Geomagnetic latitude: -1.60). Location of the FPI on map of West Africa is shown in Figure 1a, while Figure 1b is an image of the NCAR FPI in Abuja.

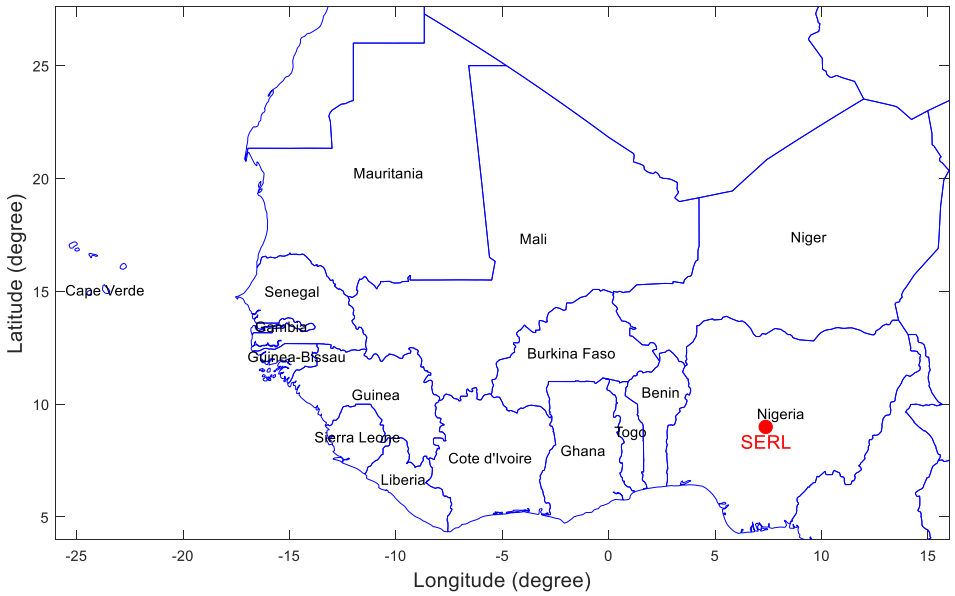

Figure 1a. Map of West Africa showing location of the Fabry-Perot interferometer (labelled SERL).

Figure 1b. Photograph of NCAR Fabry-Perot interferometer at SERL, Abuja.

The integration time is 10 minutes for the 630.0 nm emission. The entire process lasts for about 40 minutes including CCD readout time, movement times for the filter wheel, and the sky scanner. The images contain multiple orders of the 630.0 nm emission spectra collected by the FPI (Wu et al., 2004; Makela et al., 2011). Each order is analysed individually to extract the estimates of Doppler shift (neutral wind), Doppler broadening (neutral temperature), 630 nm intensity, and background continuum intensity. The individual estimates obtained from each order are averaged together, and weighted by the uncertainty of the individual estimates to obtain the final estimated parameters used here. A zero reference for the Doppler shifts must be established to obtain absolute estimates of the line-of-sight neutral wind.

It is important to note here that the FPI installed was connected to a cloud detector for sky condition monitoring. The sky cloud condition was recorded and was used to remove periods of cloud cover, which prevents the airglow emission from being observed from the ground. The FPI is mostly powered by Solar Power System to make up for power failure usually experienced in this region.

Data from the FPI instrument were obtained and stored as images. Each image is stored as a file with a 2-byte integer header. The image size is 346x258 (2-byte unsigned integer) that is a result of 4x4 binning of the CCD chip. The 4x4 binning provides sufficient resolution, at the same time, increases the sensitivity of the super bin (4x4 size). The image data are processed into wind speed information using a software developed at NCAR (Wu et al., 2004). The period of observation reported in this work during quiet conditions spanned through March, April, May and June in 2016; September, October, November and December in 2017; and January in 2018, with a useable data of 139 nights.

3. Results and Discussions

3.1. Night-time and monthly variations

Table 1 shows a summary of the monthly mean of the thermospheric wind speeds. The columns labelled 'All hours' indicate the average of wind speeds for the entire night-time duration between 19:00 local time (LT) and 05:00 LT. The 'pre-midnight (19:00 LT-23:00 LT)' and 'post-midnight (24:00 LT-05:00 LT)' hours are noted.

On average as can be observed in Table 1, the meridional winds ranged between -43 and 7 ms^{-1} and the zonal winds are between 19 and 85 ms^{-1}. In these cases of meridional wind, they are more equatorward in the post-midnight sector prior to 05:00 LT than the pre-

144 midnight. These were further confirmed in Figures 3a and 3b as the monthly average of
145 meridional wind magnitudes during post-midnight are generally less than those ones of pre-
146 midnights. For zonal wind, stronger eastward flow was obvious in all of these months at the
147 beginning of the nights compared to their post-midnights. Similar varying pattern was
148 obvious in Figure 4a and 4b with regards to all of the monthly averages investigated with
149 an exception in April 2016.
150
151 **Table 1.** Summary of the monthly mean of the thermospheric wind speeds (ranges are in
152 parenthesis) - all components are measured in ms^{-1}

Month	**All Hours**		**Pre-midnight Hours**		**Post-midnight Hours**	
	Meridional	**Zonal**	**Meridional**	**Zonal**	**Meridional**	**Zonal**
Mar 2016	0.43 (188.30)	85.05 (322.80)	-13.01 (188.30)	76.51 (322.80)	17.65 (39.28)	94.21 (223.85)
Apr 2016	-14.77 (153.88)	85.33 (203.58)	-19.05 (153.88)	105.20 (159.62)	-13.03 (101.26)	51.05 (203.58)
May 2016	-0.39 (230.14)	31.92 (248.19)	7.36 (163.89)	61.63 (107.61)	-8.57 (173.94)	13.94 (62.67)
Jun 2016	3.63 (331.77)	75.25 (339.86)	14.34 (98.56)	113.39 (125.16)	-15.37 (331.77)	11.36 (276.14)
Sep 2017	-2.75 (341.82)	49.60 (181.91)	-9.54 (148.37)	48.49 (170.95)	-2.05 (341.82)	49.07 (169.06)
Oct 2017	7.05 (117.39)	44.82 (181.01)	2.79 (53.96)	63.81 (71.96)	12.73 (117.39)	27.68 (148.43)

Nov 2017	5.11 (171.86)	58.83 (87.85)	9.14 (151.93)	55.78 (87.85)	3.00 (133.71)	62.84 (43.16)
Dec 2017	-42.48 (109.24)	77.47 (370.56)	-45.93 (109.24)	83.73 (245.19)	-33.52 (76.50)	71.41 (205.12)
Jan 2018	-6.16 (278.57)	19.33 (239.07)	-32.37 (236.61)	52.59 (238.96)	24.01 (213.23)	-19.72 (134.55)

Figure 2 shows a 30-minute time resolution of night-time variation of meridional and zonal winds speeds for some months in year 2016, 2017 and 2018. These years of study belong to the decline stage of solar-cycle 24 (solar minimum). In 2016, data spanned from March through June; 2017 had useable data from September to December, and in 2018, only January data was available. The upper panel of Figure 2 shows the meridional wind variations while the lower panel represents the zonal wind variations.

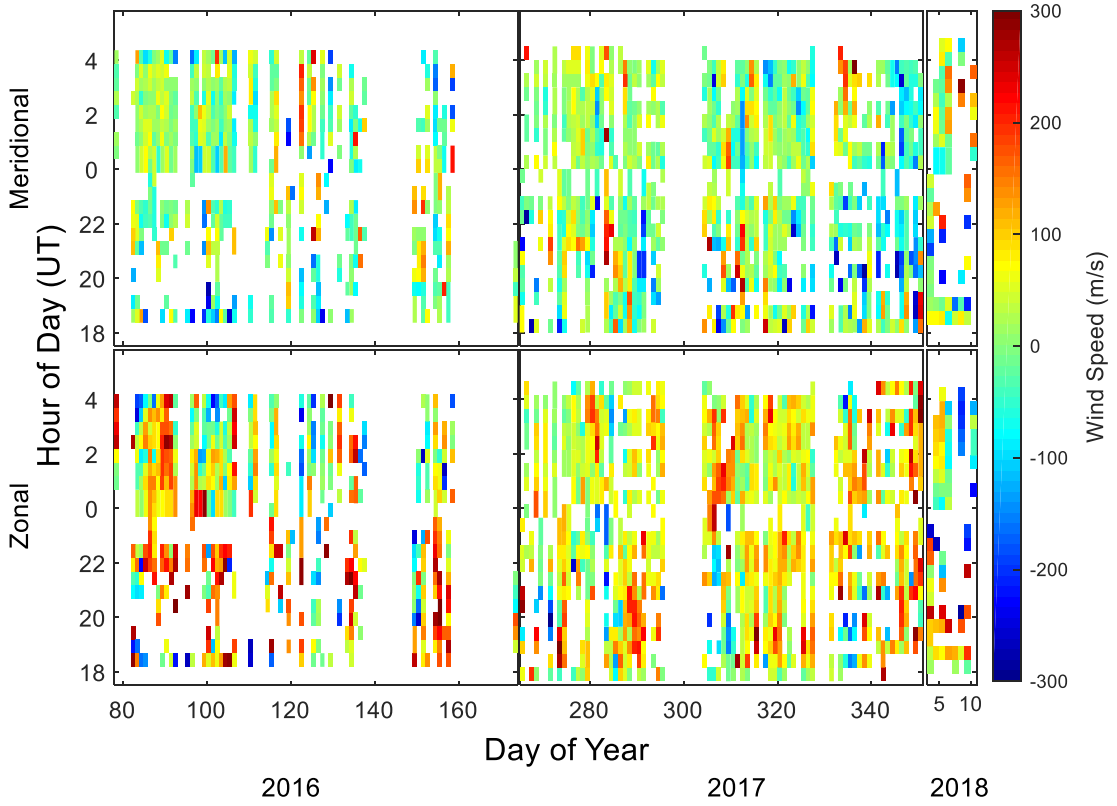

161

162 **Figure 2.** Night-time speeds of the varying meridional and zonal winds for year 2016-2018
163 (The upper panel shows the meridional wind and the lower panel represents the zonal
164 wind).

165 For all of the varying meridional winds investigated (upper panel in Figure 2), the
166 maximum values vary between ~ 150 and ~ 200 ms^{-1}. The zonal component (lower panel of
167 Figure 2) shows different degrees of variability in speed during all nights. For example in
168 March-April 2016, the dominating eastward varying zonal wind between pre-midnight
169 (~23:00 LT) and the early pre-dawn (~ 02:00 LT) period reached up to ~ 250 ms^{-1}.
170 Figures 3a and 3b show the monthly average of meridional winds (red lines). The hourly
171 standard deviation in the statistical monthly average analysis of these data are represented
172 with the vertical error bars. These available data in year 2016 are able to unveil two

seasons; March equinox (March and April) and June solstice (May and June). Also, data for year 2017 unveiled two seasons; September equinox (September and October) and December Solstice (November and December). For January 2018, it is part of year 2017 December season.

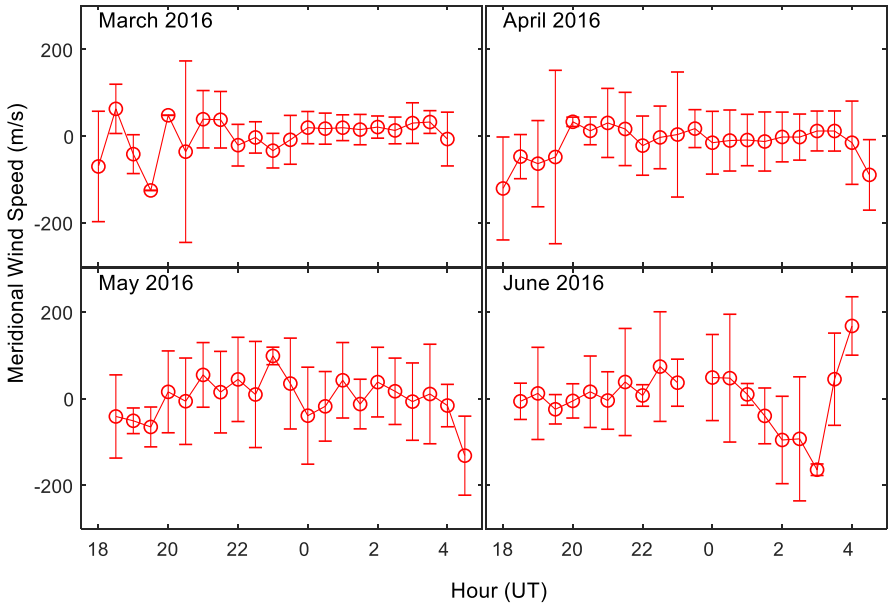

Figure 3a. Night-time variation of the speed of the meridional wind in 2016 (the vertical error bars indicate the standard deviations of the observations binned in 30-minute interval)

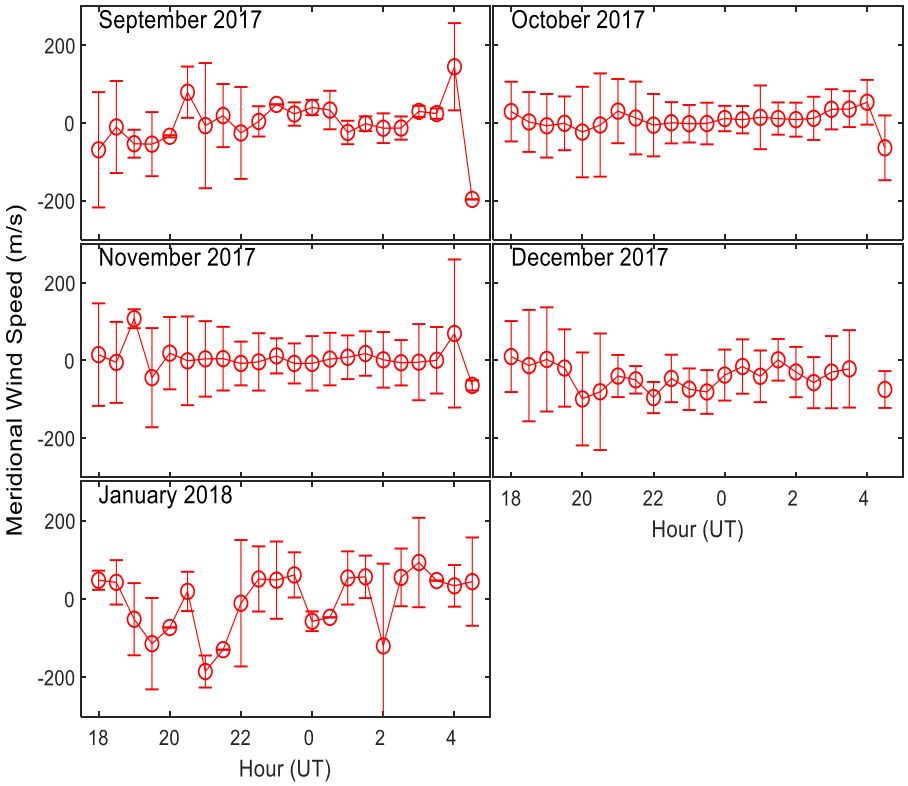

Figure 3b. Night-time variation of the speed of the meridional wind in 2017-2018 (the vertical error bars indicate the standard deviations of the observations binned in 30-minute interval)

We observed some interesting longitudinal differences with regards to meridional winds during March-April 2016, which coincided with the periods of investigation in the works of Tesema et al. (2017). One of these longitudinal differences seen in our results (an equatorial West African station) is a strong poleward movement of meridional wind varying between ~ 100 ms^{-1} and ~ 180 ms^{-1} in the early evening (around 19:00 LT-21:00 LT). These contrast Tesema et al. (2017) reports of a less/weak poleward (equatorward) movement of meriodinal winds in the early evening of March-April 2016 in Ethiopia, an equatorial station in East Africa. After 21:00LT, our results revealed further contrasting feature as abatement of poleward movement of meridional wind gradually evolved into an

195 equatorward movement and fluctuated around ~ 0-10 ms^{-1} through the midnight until 04:00
196 LT. These weak speeds in equatorward meridional winds can be responsible for the
197 absence of midnight temperature maximum (MTM) in equatorial West Africa in March-
198 April 2016. However, moderate increase in equatorward meridional wind speed, which can
199 be linked with MTM was obvious in January 2018 around local midnight as its southward
200 poleward movement in the early evening times contrasts Tesema et al. (2017) results.
201 Earlier before now, Batista et al. (1997) and Meriwether et al. (2008) had reported a surge
202 in the MTM, which was associated with a surge in equatorward meridional wind speed
203 around local midnight (Colerico et al., 2006; Tesema et al., 2017).
204 Throughout the nights of May 2016, meridional wind speed oscillates between both the
205 poles and the equator with a somewhat constant inter-hour variability. The month of June
206 2016 exhibits contrasting characteristics compared to that of March-April 2016 in that,
207 prior to midnight, the meridional wind was majorly equatorward after which it surged and
208 became poleward with a speed ~140 ms^{-1}.
209 With September 2017 as an exception, there is a weak poleward meridional wind in the
210 evening periods of November and December 2017. Later on and prior to 05:00 LT,
211 equatorward meridional wind became obvious. This weak monthly average of poleward
212 meridional wind seen in our results contrast those ones reported by Tesema et al. (2017) in
213 November and December 2016 as theirs are characterized by a strong poleward meridional
214 wind. In the case of September 2017 in the early evening period over equatorial West
215 Africa, a strong varying monthly average poleward meridional wind was southward. Also
216 for record purposes, the monthly average varying meridional wind of October 2017 was
217 equatorward from evening period until 05:00 LT. As can be observed (Figure 3b), a

meridional wind speed that reached its maximum value later on at 05:00 LT in September 2017 (~ 200 ms^{-1}) and October 2017 (~ 60 ms^{-1}) was earlier in November 2017 (~ 130 ms^{-1}) and December 2017 (~ 100 ms^{-1}) at 20:00 LT and 21:00 LT, respectively. A similar morphology in the varying thermospheric neutral meridional wind have been reported in the works of Meriwether et al. (2011) at Cajazeiras (Brazil). They found that a maximum meridional wind speed was reached earlier in December solstice when compared to those ones of equinoctial months (October and February).

The variability of the monthly-averaged values of the zonal wind is presented in Figures 4a and 4b (blue lines). The monthly variation in the zonal component shows a predominantly eastward wind in most of the hours, months, seasons and years considered. This is typical of a low latitude ionosphere (Richmond et al., 1992; Batista et al., 1997). The trend of these variations is a gradual increase in magnitude from twilight to dusk and followed by a decrease near midnight hours. The high value of varying zonal wind reported by Tesema et al. (2017) at the early hours of the night in March-April 2016 was repeated in our results. But, ours have higher values in the range of ~ 180 – 239 ms^{-1} compared to theirs in the range of ~ 50- 100 ms^{-1}. The exceptions seen in March-April 2016 that also contrast the works of Tesema et al. (2017) are near midnight increase in the varying zonal wind (~ 150-200 ms^{-1}). A near-stable and least speed of ~ 88 ms^{-1} was seen in October and November 2017.

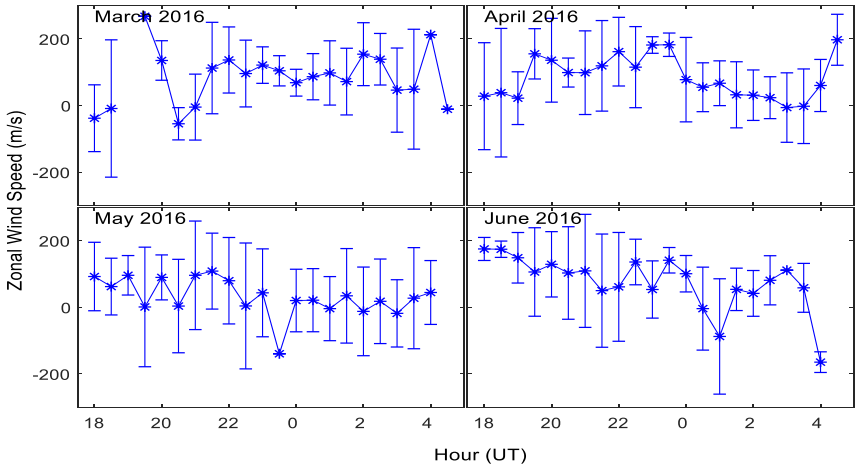

238

239 **Figure 4a.** Night-time variation of the zonal wind speed in 2016 (the vertical error bars
240 indicate the standard deviations of the observations binned in 30-minute interval).

241

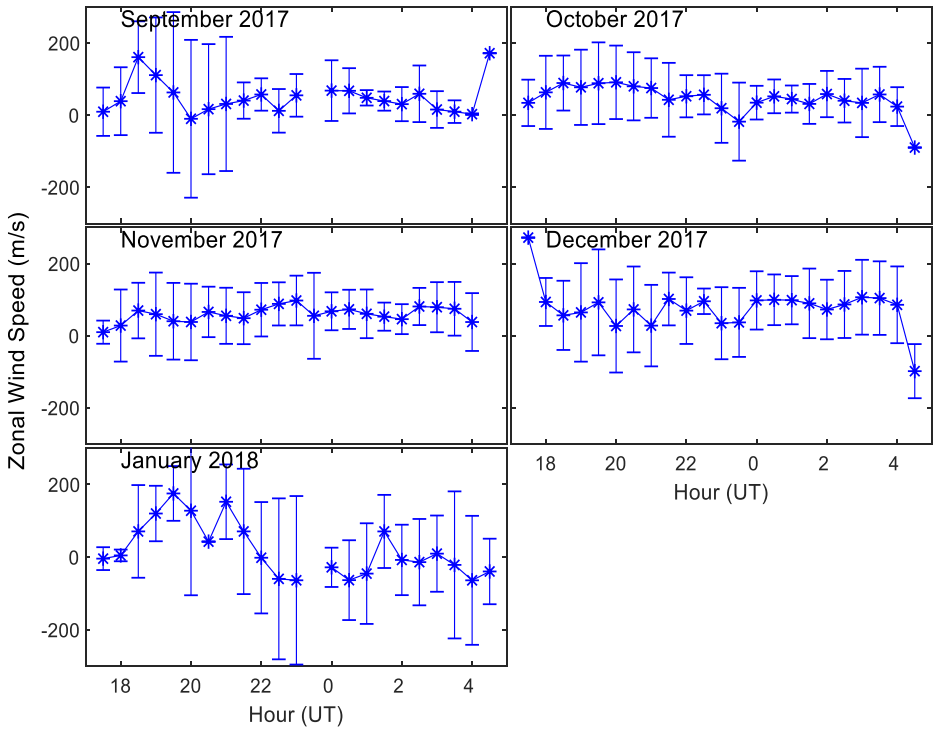

242

243 **Figure 4b.** Night-time variation of the zonal wind speed in 2017-2018 (the vertical error
244 bars indicate the standard deviations of the observations binned in 30-minute interval).
245

These gradual increase and enhancements exhibited by the eastward zonal wind across all these months and seasons during the early hours of the night is a strong indication of reduced ion drag in the F-region. This was due to a strong eastward zonal wind around the geomagnetic equator in the early hours of the nights (Richmond et al., 1992). It is important to recall that a strong pre-reversal enhancement in electric field dynamo just after the sunset lifts the F region plasma to higher altitudes (Batista et al., 1997), making the F- region becomes very active. This therefore suggests that the pre-reversal enhancement in electric field could be due to this strong eastward wind just after sunset.

It is interesting to put forward from Table 2 for record purposes that the varying zonal and meridional winds observed in this work over West Africa are higher when compared to all of the other works that have been investigated in other stations around the world (Martinis et al., 2001; Meriwether et al., 2011; Makela et al., 2013; Tesema et al., 2017 and Malki et al., 2018). In addition to Table 2, the results we have presented above confirm that there are many significant changes in the varying thermospheric neutral (zonal and meridional) wind between the West (Nigeria) and East (Ethiopia) Africa equatorial stations. As these significant changes seen in these varying thermospheric neutral winds are interacting with the upward propagating tides in the thermosphere, the equatorial electric fields and the vertical distribution of plasma in the low latitudes can be significantly modulated. These justified the suggestions of Jones et al. (2013) and Maute et al. (2015) with regards to the effect of thermospheric neutral winds coupling ions. We therefore conclude that these significant changes seen in these thermospheric neutral winds are the reason for the longitudinal differences that have been reported in equatorial electric fields between the West and East Africa stations (Rabiu et al., 2011; 2017; Yizengaw et al., 2014; Bolaji et al.,

2016). The reality is that the geomagnetic main fields with respect to the dip equator over the West and East Africa are both almost horizontal.

Table 2. Comparison of the thermospheric wind speeds obtained in this work with those of other regions from existing literatures.

Sector	Max zonal wind ms^{-1}	Max meridional wind ms^{-1}	References
West Africa*	271.83	196.99	This work
East Africa	90	50	Tesema et al., 2017
Morocco, North Africa	80	120	Malki et al, 2018
Peruvian	150		Martinis et al., 2001;Meriwether et al., 2011, 2012).
Brazilian	100		Meriwether et al., 2012;Makela et al., 2013

The monthly varying values of thermospheric winds shown with bar chart in Figure 5 represent the seasonal variability between both wind components for the period under study. As previously observed in the investigation over Ethiopia (Tesema et al., 2017) and Norway (Xu et al., 2019), our results (Figure 5) confirm that the meridional component is usually slower than the zonal component (Portnyagin and Solovjova, 1999).

Figure 5 shows a strong and interesting seasonal variability between the maximum monthly values of both components of the thermospheric winds for the period under study. The monthly maximum value was identified for each month for both wind systems. As previously observed in the study over Ethiopia (Tesema et al., 2017), and also in Norway (Xu et al., 2019), the meridional component is usually about ~2 times slower than the zonal component (Portnyagin and Solovjova, 1999) owing to the fast response of zonal winds to

increasing plasma convection (Xu et al., 2019). As such, the maximum zonal wind speed of 271.91 ms^{-1} was obtained in December 2017 followed by 268.17 ms^{-1} in March 2016; while the maximum meridional wind of 196.99 ms^{-1} was obtained in September 2017. Incidentally, both the meridional and zonal wind recorded the least values of 64.1 ms^{-1} and 90.81 ms^{-1} respectively in the same month of October 2017. These variability patterns have been reported in the works of Emmert et al. (2006).

The peaks of the meridional wind increased gradually from March to June 2016 as similarly detected in Emmert et al. (2006), while the magnitude of the zonal wind collapses gradually during this same period with an exception found in June. After the Equinox month in 2017, both the meridional and zonal component decreased sharply to ~60 ms^{-1} and ~90 ms^{-1} respectively. A similar observation was made over North-eastern Brazil (Fisher et al., 2015) when the zonal wind rapidly reduced towards zero especially in the local summer months. In the region of this current study, October marks the commencement of the dry season, and so referred to as the “local summer”. Similarly, Emmert et al., (2006) investigated over 7 sites (Arequipa, Peru inclusive) on how the magnitude of the zonal and meridional components might be impacted by solar extreme ultraviolet (EUV) irradiance and the day of the year - it was found out that over some sites, the wind speeds is smallest at solar maximum. Thus, the intense winds from 2016-2018 are observed as a result of measurements taken close the solar minimum.

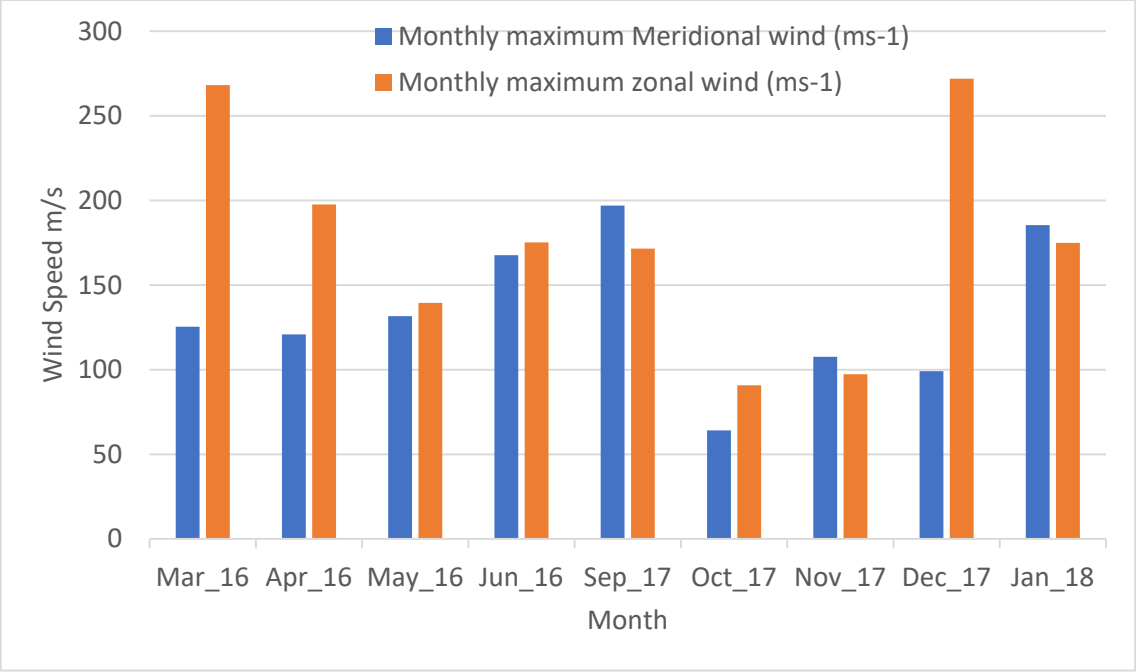

Figure 5. Variation of the maximum monthly values of the thermospheric winds

After September (an equinoctial month) in 2017, both the meridional and zonal components decreased sharply in October 2017 to ~ 65 ms^{-1} and ~90 ms^{-1}, respectively. A similar significant reduction closer to zero in the varying zonal wind observation have been reported over North-Eastern Brazil in the local summer months (Fisher et al., 2015). It is important to note that October marks the commencement of the dry season in Nigeria, and so referred to as the "local summer". It is also important to recall that Emmert et al. (2006) investigated the response of zonal and meridional components to the impact of solar extreme ultraviolet (EUV) irradiance in all months over 7 stations in South American sector. Their findings revealed similar smallest winds speeds at solar maximum. This could be one of the reasons for significant increase in wind components closer to solar minimum as seen in our result from 2016 to 2018.

3.2. Comparison of observed neutral wind speeds with values from the horizontal wind model (HWM)

Figures 6 and 7 show results of the comparisons between observed thermospheric neutral wind speeds and corresponding values from the horizontal wind model-14 (HWM-14). The HWM describes statistical behaviours of neutral winds from the surface to about 500 km and has been continuously updated based on a wide range of observed data and theoretical consideration (Hedin et al., 1988). The HWM14 is the most recent version which has been updated with thermospheric observations by including additional ground-based FPI measurements from 630 nm airglow emission and GOCE satellite data. This is to ensure better descriptions (Drob et al., 2015). The HWM neutral wind speeds used in this work are values for altitude 250 km.

Referencing Figure 6a which compares the meridional measurements with those of HWM-14 in March-June 2016, a good agreement was observed just after 23:00 LT as both measurements steadily increased until 04:00 LT. In May, HWM-14 display good prediction of the varying meridional wind from midnight until 05:00 LT. However, the correlation between the HWM-14 and the measurement is quite low for the pre-midnight hours. The exception seen in June 2016 was a sharp decrease in the observed varying meridional wind around 02:00 LT compared to the increasing HWM-14 measurements.

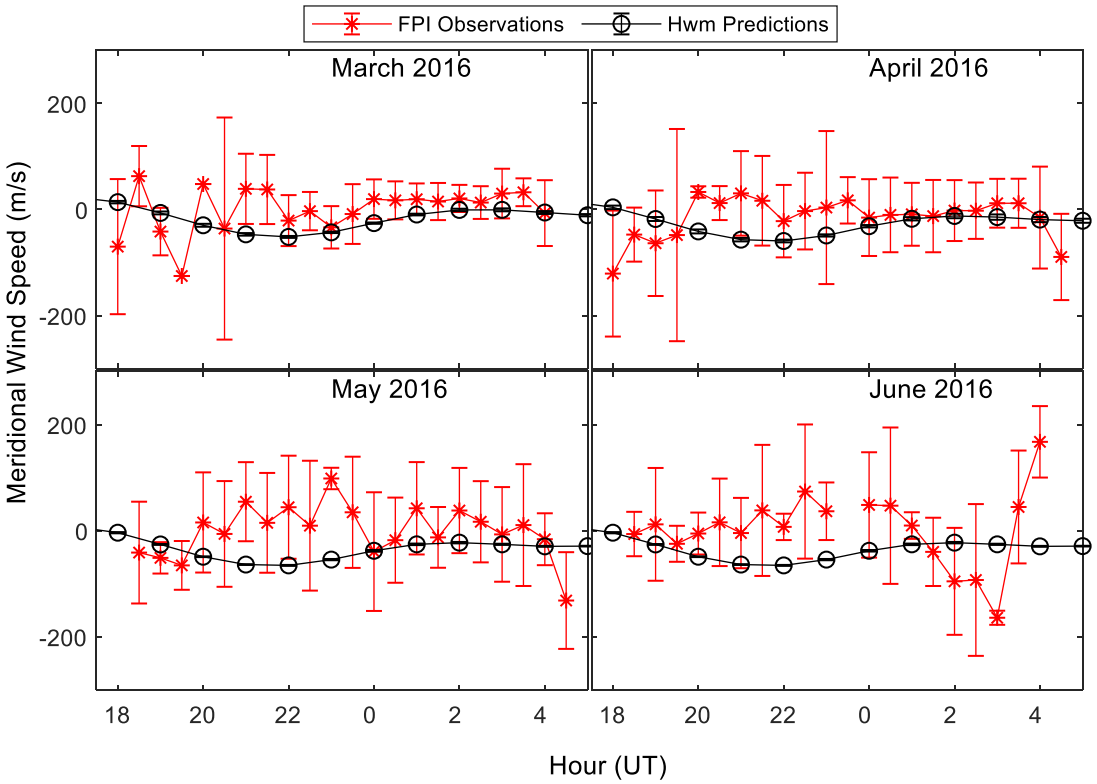

337

338 **Figure 6a.** Comparison of the observed meridional wind speeds (red lines with asterisked
339 points) with the HWM model values (black lines with circled points) for March to June
340 2016.

341

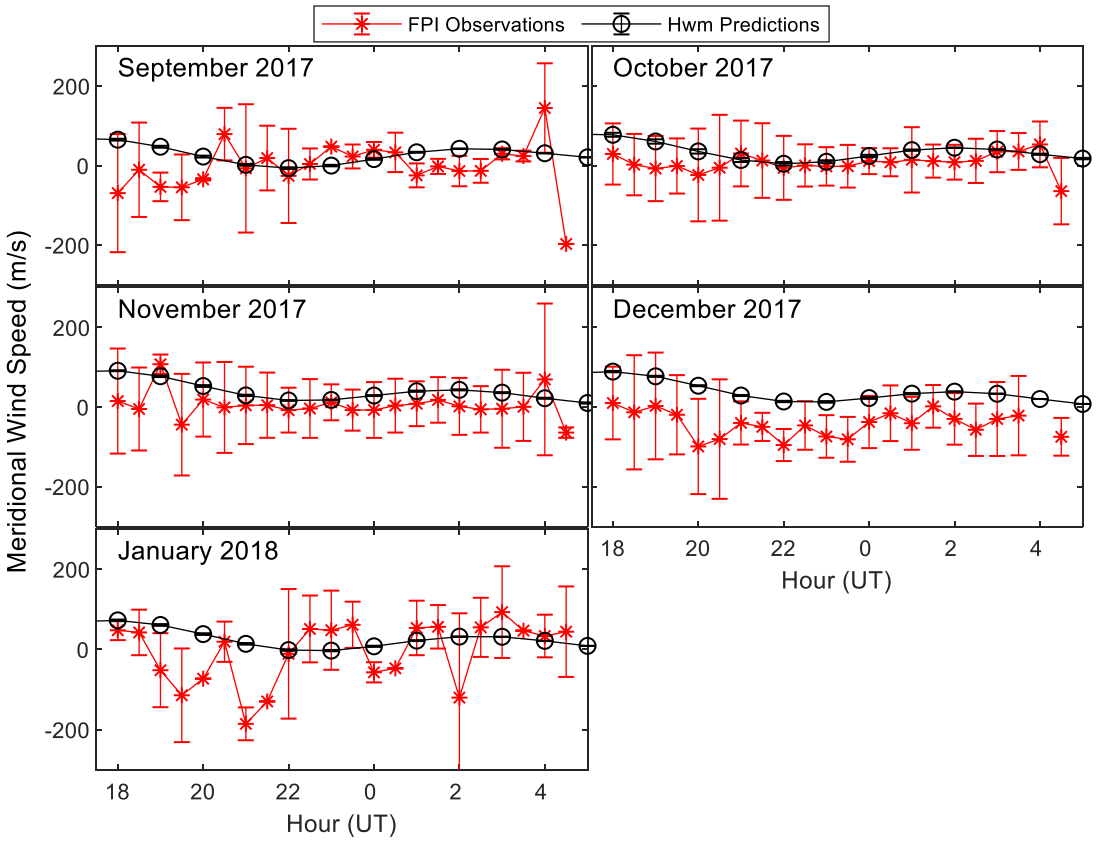

342

343 **Figure 6b.** Comparison of the observed meridional wind speeds (red lines with asterisked
344 points) with the HWM model values (black lines with circled points) for September 2017 to
345 January 2018.

346

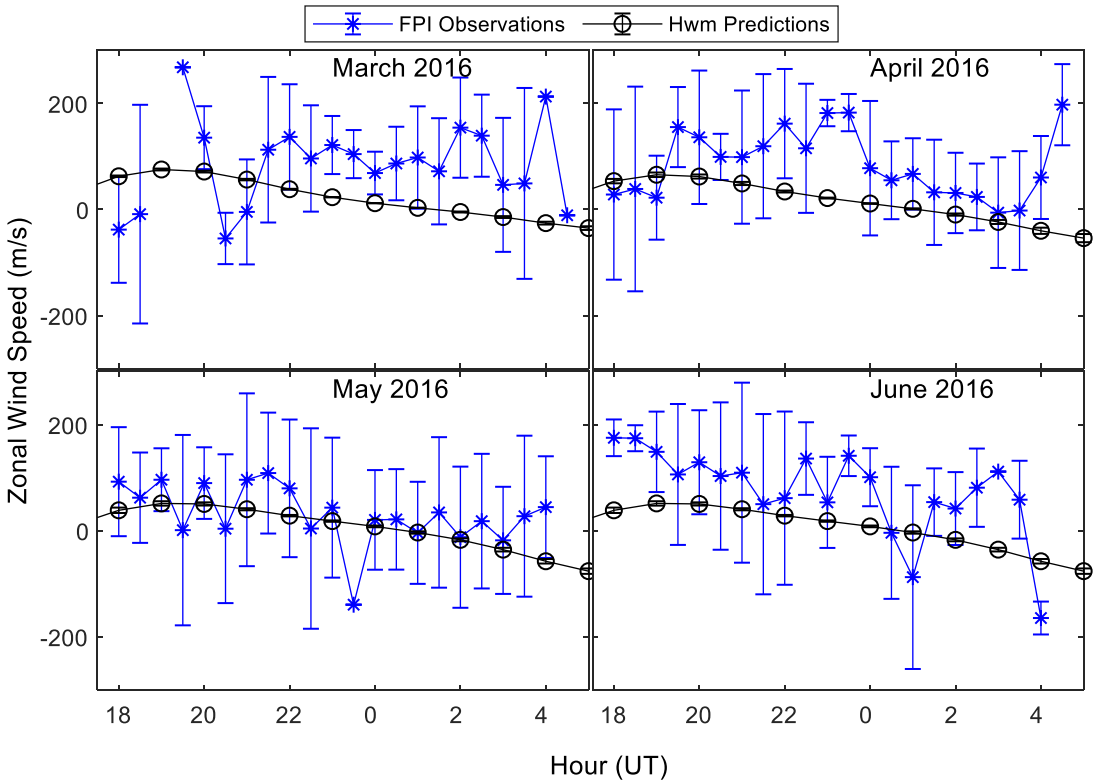

347

348 **Figure 7a.** Comparison of the observed zonal wind speeds (blue lines with asterisked
349 points) with the HWM model values (black lines with circled points) for March to June
350 2016.

351

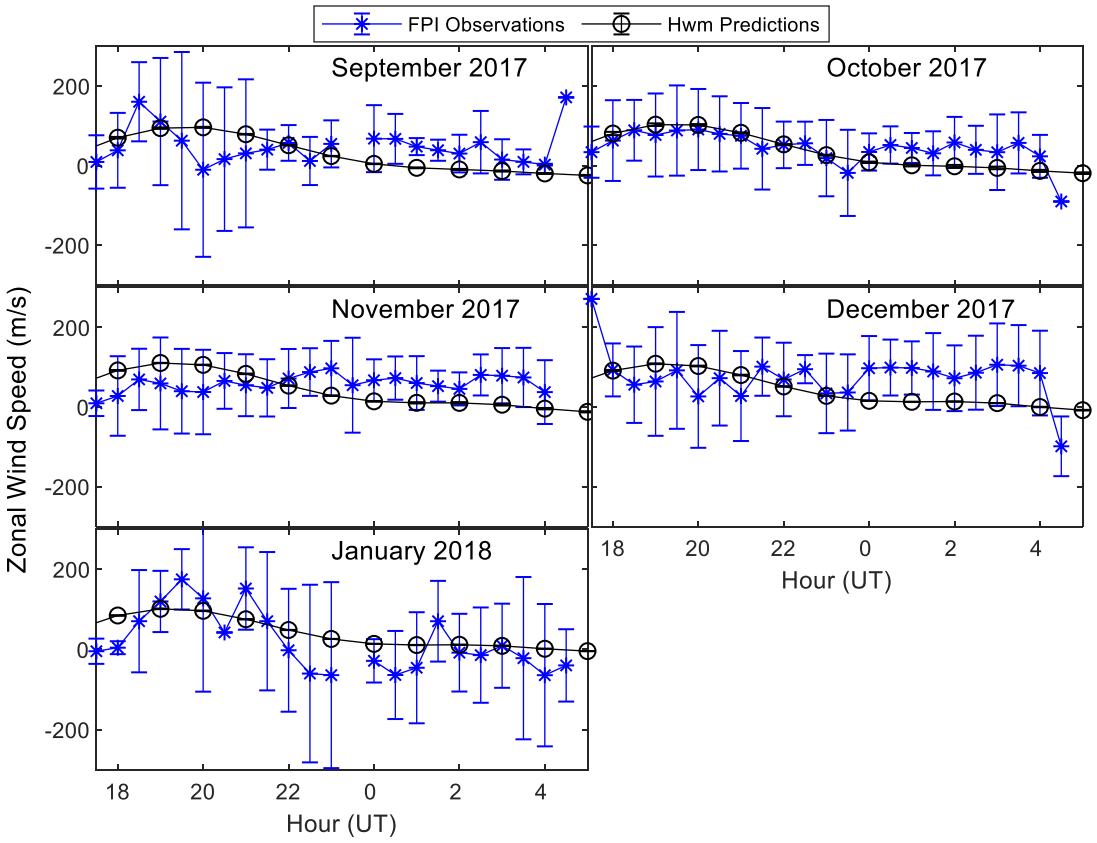

Figure 7b. Comparison of the observed zonal wind speeds (blue lines with asterisked points) with the HWM model values (black lines with circled points) for September 2017 to January 2018.

In this June 2016, there is a negative correlation in the early evening; in the early evening of the 2016 months, the HWM-14 did not reproduce accurately the wind values as tremendous under-estimation was observed. With an exception of December 2017 that was over-predicted by HWM-14 in the early evening, it generally gives a good prediction of the meridional winds. In Figure 7a, the model correctly simulated the attempting westward trend of the zonal wind measurements from 19:00 LT until 04:00 LT. Although, it underestimated the wind speeds and does not properly capture the oscillations. The estimates of the varying zonal winds for the months in 2017 closely agree with the

365 experimental measurements in terms of magnitudes and signatures, even though, higher
366 wind values are measured by the FPI after midnight.

367 **3.3. Periods associated with the thermospheric winds**

368 Figures 8 and 9 demonstrate periodicities associated with thermospheric winds. The
369 illustrated periodograms are obtained with a MATLAB-based Fast Fourier Transform
370 (FFT) technique using thermospheric wind daily maximum speeds as inputs. Table 3
371 highlights the periods of oscillation exhibited by the winds as explained, in parentheses, in
372 the figure captions. The zonal wind (in Figures 8a and 8b) manifested modal periods of
373 25.9 and 133.5 days which are quasi 27-days and quasi terannual periodic variations
374 respectively. While the meridional wind (in Figures 9a and 9b) only manifested oscillatory
375 period of 133.5 and 23.1 days in the year 2016 and 2017 respectively. With regards to
376 zonal wind, the periodicity of 133.5 days per cycle was obvious in year 2016 and 2017-
377 January 2018. In meridional wind, it appeared only in year 2016 data. Many works,
378 including those of Altadill et al. (2001), Altadill and Apostolov (2003), and Pancheva et al.
379 (2002) had reported the presence of a 27-day oscillation in the ionosphere. Kutiev et al.
380 (2012) emphasised that quasi-27-day periodicity is a typical medium-term response of the
381 ionosphere to changes in solar and geomagnetic activity. The main factor generating such
382 changes is the repeatable influence of active regions on the Sun's surface which rotates
383 with a period of 27 days. The 27-day solar rotation is a characteristic periodicity in EUV
384 flux that has been clearly correlated to changes in the density of the thermosphere (Thayer
385 et al., 2008). Terannual and 27-day periodicity were among the periods reported by Manson
386 et al. (1981) in thermospheric winds at Saskatoon. Xu et al. (2012) found a terannual
387 periodic oscillation in F2 layer peak electron density (NmF2) which vary with solar activity

388 in the same way. Reid et al. (2014) reported a terannual oscillation in the night-time OI
389 airglow intensity at Adelaide. The zonal winds generally exhibited weak magnitude on
390 most of the nights. Few nights recorded speeds of ~150 ms^{-1}.

391

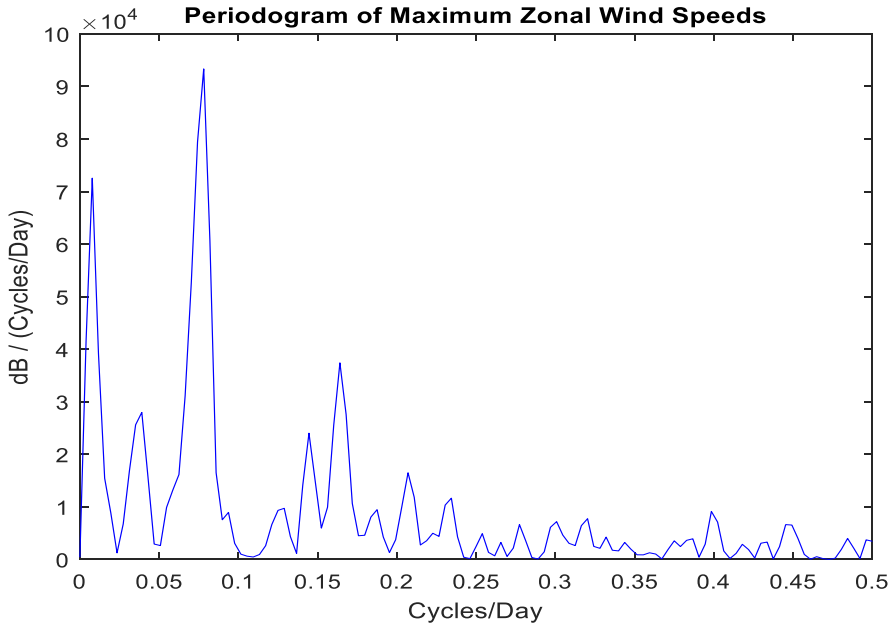

392

393 **Figure 8a.** Periodogram showing the periods associated with zonal wind daily maximum
394 amplitude for the year 2016 (the top 5 peaks show periodicities at around 0.0781, 0.0075,
395 0.1642, 0.0386, and 0.1446 cycles per day, corresponding to 12.8, 133.5, 6.1, 25.9, and 6.9
396 days per cycle).

397

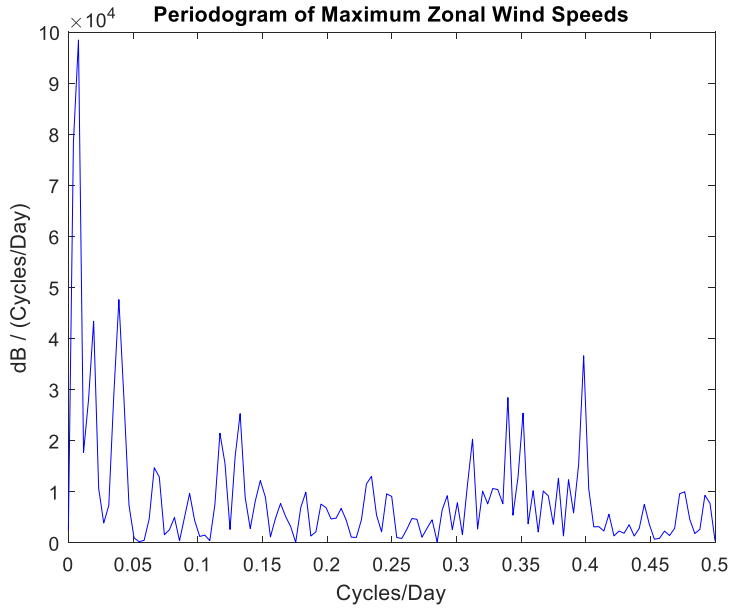

Figure 8b. Periodogram showing the periods associated with zonal wind daily maximum amplitude for the year 2017-Jan 2018 (the top 5 peaks show periodicities at around 0.0075, 0.0386, 0.0190, 0.3980, and 0.1331 cycles per day, corresponding to 133.5, 25.9, 52.6, 2.5, and 7.5 days per cycle).

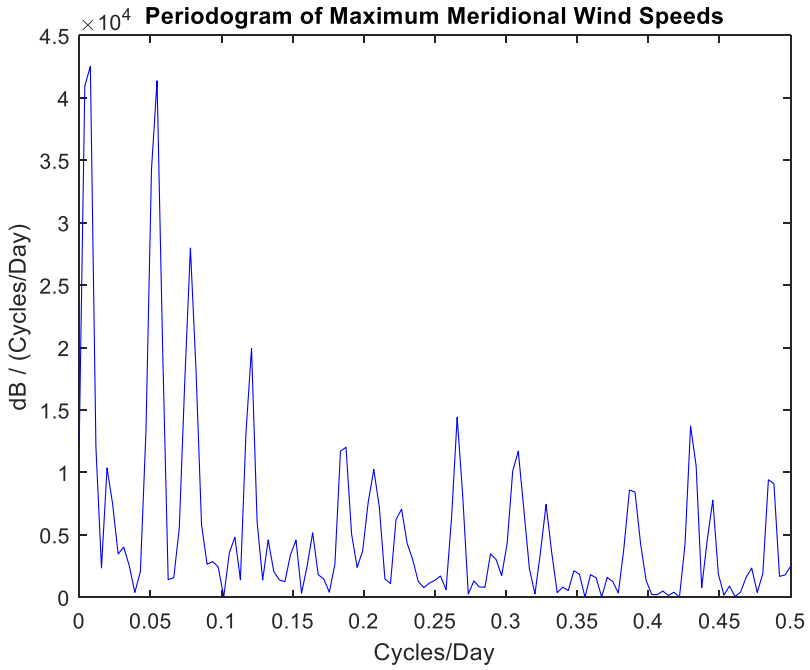

Figure 9a. Periodogram showing the periods associated with meridional wind daily maximum amplitude for the year 2016 (the top 5 peaks show periodicities at around

0.0075, 0.0547, 0.0778, 0.1204, and 0.2656 cycles per day, corresponding to 133.5, 18.3, 12.9, 8.3, and 3.8 days per cycle)

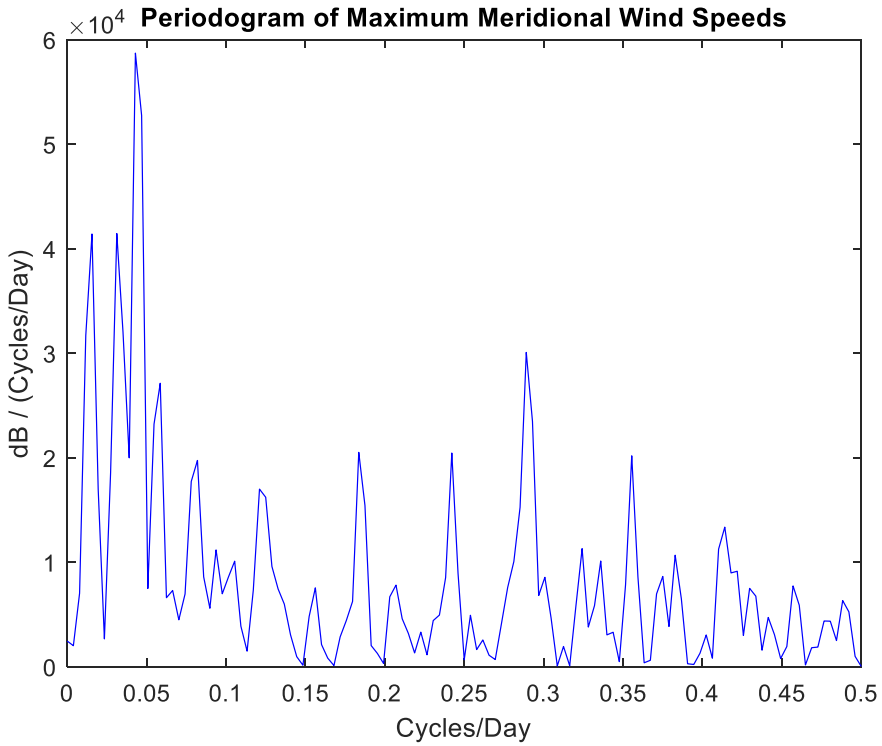

Figure 9b. Periodogram showing the periods associated with meridional wind daily maximum amplitude for the year 2017-Jan2018 (the top 5 peaks show periodicities at around 0.0432, 0.0156, 0.0305, 0.2886, and 0.0582 cycles per day, corresponding to 23.1, 64.3, 32.8, 3.5, and 17.2 days per cycle)

Table 3. Periods associated with the thermospheric winds

Wind	**Period (days)**	
	2016	2017- January 2018
Zonal Wind	6.1, 6.9, 25.9, 12.8, 133.5	2.5, 7.5, 25.9, 52.6, 133.5
Meridional Wind	3.8, 8.3, 12.9, 18.3, 133.5,	3.5, 17.2, 23.1, 32.8, 64.3

4. Conclusions

This work investigated the variability of night-time equatorial thermospheric winds observed by an optical Fabry–Perot Interferometer (FPI). The FPI observations from March 2016 to January 2018 with 139 nights of good data are employed. Some of our results shared some similarities with some studies already done in other sectors. For example, the varying zonal winds are predominantly eastwards in all months. Other interesting findings of this study can be summarized as follows:

1. The magnitude of the thermospheric winds observed in this study (West African sector) is much stronger than those ones that have been reported in other longitudinal sectors. Compared to the higher zonal wind speed (~ 150 ms^{-1}) reported in Peruvian sector (Martinis et al., 2001; Meriwether et al., 2011, 2012), we observed ~ 272 ms^{-1}. And for our meridional wind speed of ~ 197 ms^{-1} during quiet conditions, it was higher than ~ 50 ms^{-1} observed in East Africa (Tesema et al., 2017).

2. There is high hour-to-hour variability in both the magnitude and direction of the meridional and zonal winds. The meridional wind was majorly poleward in the early evening of March-June 2016 and September-November 2017. It remains equatorwards at other periods with an inherent stability observed in the months of 2017.

3. The spectral analysis of the daily maximum values revealed that the zonal winds manifested modal periods of 25.9 and 133.5 days, which are quasi 27-days and quasi terannual periodic variations, respectively. While the meridional wind manifested oscillatory periods of 133.5 and 23.1 days among others in the year 2016 and 2017, respectively.

4. The performance assessment of the HWM-14 model revealed that the temporal and seasonal dynamics of both the zonal and meridional winds were properly reproduced in 2017. In 2016, with the exception of March and April, the model underestimated the meridional wind speeds as it did in the zonal winds even though the temporal evolution was well captured.

This study provided insights into the behavioural pattern of thermospheric winds and the representativeness of the HWM14 empirical model over the West Africa sector. Hence, this calls for the improvement of the model by using newly observed measurements over this region in order to improve its performance to produce more realistic estimations. This would also increase data availability and expand the knowledge base about thermospheric winds in low latitudinal sectors that are without ground-based instruments.

Acknowledgements

The Fabry-Perot interferometer FPI installed in Abuja was deployed by the US National Center for Atmospheric Research (NCAR) with US National Science Foundation (NSF) research grant. Maintenance and operation of the FPI at the Space Environment Research Laboratory, Abuja has been supported by Centre for Atmospheric Research using R & D fund from the Federal Government of Nigeria. FPI dataset used in this work is available at https://carnasrda.com/fpi_data/. We thank developers of the HWM for making the model available. The HWM is available at https://ccmc.gsfc.nasa.gov/modelweb/atmos/hwm.html.

References

Altadill, D., E. M. Apostolov, J. G. Sole, and C. Jacobi (2001). Origin and development of vertical propagating oscillations with periods of planetary waves in the ionospheric F region, Phys. Chem. Earth, Part C, 26(6), 387–393.

Altadill, D., and E. M. Apostolov (2003). Time and scale size of planetary wave signatures in the ionospheric F region: Role of the geomagnetic activity and mesosphere/lower thermosphere wind, J. Geophys. Res., 108(A11), 1403, doi:10.1029/2003JA010015.

Batista, I., Sastri, J., Medeiros, R. and Abdu, M. (1997). Nighttime thermospheric meridional winds at Cachoeira Paulista (23°S, 45°W): Evidence for effects of the equatorial midnight pressure bulge. Journal of Geophysical Research. 102. 20059-20062. 10.1029/97JA01387.

Bolaji., O.S, Owolabi, O. P, Falayi, E. Jimoh, E, Kotoye, A, Odeyemi, O, Rabiu, O, Doherty, P, Yizengaw, E, Yamazaki, and Onanuga, O, K (2016). Solar quiet current response in the African sector due to a 2009 sudden stratospheric warming event, Journal of Geophysical Research: Space Physics, 121, doi:10.1002/2016JA022857.

Burnside R. G., Herrero, F. A., Meriwether Jr., J. W., and Walker, J. C. G. (1981). Optical Observations of Thermospheric Dynamics at Arecibo, J. Geophys. Res., 86, 5532–5540.

Colerico, M. J., Mendillo, M., Fesen, C. G., and Meriwether, J. (2006). Comparative investigations of equatorial electrodynamics and low-to-mid latitude coupling of the thermosphere-ionosphere system, Ann. Geophys., 24, 503–513, doi:10.5194/angeo-24503-2006.

Dellinger, J. H., 1939. The role of the ionosphere in radio-wave propagation, Trans. Am. lnst. Elec. Engrs. 58, 803.

Drob, D. P., Emmert, J. T., Meriwether, J. W., Makela, J. J., Doornbos, E., Conde, M., Hernandez, G., Noto, J., Zawdie, K. A., McDonald, S. E., Huba, J. D.,Klenzing, J. H. (2015). An update to the horizontal wind model (HWM): The quiet time thermosphere. Earth and Space Science, 2,301–319, doi: 10.1002/2014EA000089.

Emmert, J. T., Faivre, M. L., Hernandez, G., Jarvis, M. J., Meriwether, J. W., Niciejewski, R. J., Sipler, D. P., and Tepley, C. A. (2006). Climatologies of nighttime upper thermospheric winds measured by ground-based Fabry-Perot interferometers during geomagnetically quiet conditions: 1. Local time, latitudinal, seasonal, and solar cycle dependence, J. Geophys. Res., 111, A12302, doi:10.1029/2006JA011948.

Fisher, D. J., Makela, J. J., Meriwether, J. W., Buriti, R. A., Benkhaldoun, Z., Kaab, M., and Lagheryeb, A. (2015). Climatologies of nighttime thermospheric winds and temperatures from Fabry-Perot interferometer measurements: From solar minimum to solar maximum, *J. Geophys. Res. Space Physics*,120, 6679– 6693, doi:10.1002/2015JA021170.

Hedin, A. E., N. Spencer, and T. Killeen (1988). Empirical global model of upper thermosphere winds based on atmosphere and dynamics explorer satellite data, *J. Geophys. Res.*, **93**(A9), 9959– 9978, doi:10.1029/JA093iA09p09959.

Jones, M., Jr., J. M. Forbes, M. E. Hagan, and A. Maute (2013). Non-migrating tides in the ionosphere-thermosphere: In situ versus tropospheric sources, J. Geophys. Res. Space Physics, 118, 2438–2451, doi:10.1002/jgra.50257.

Killeen, T. L., and P. B. Hays (1984). Doppler line profile analysis for a multichannel Fabry-Perot interferometer, Applied Optics, 23 (4), 612, doi: 10.1364/AO.23.000612.

Kutiev, I., Y. Otsuka, D. Pancheva, and R. Heelis (2012). Response of low-latitude ionosphere to medium-term changes of solar and geomagnetic activity, J. Geophys. Res., 117, A08330, doi:10.1029/2012JA017641.

Makela, J. J., Fisher, D. J., Meriwether, J. W., Buriti, R. A., andMedeiros, A. F. (2013). Near-continual ground-based nighttime observations of thermospheric neutral winds and temperatures over north eastern Brazil from 2009–2012, J. Atmos. Sol. Terr. Phys.,103, 94–102, doi:10.1016/j.jastp.2012.11.019.

Malki, K., Bounhir, A., 1,Benkhaldoun, Z., Makela, J. J., Vilmer, N., Fisher D. J., Kaab, M., 1,Elbouyahyaoui, K., Harding, B. J., Laghriyeb, B., Daassou, A., Lazrek, M., (2018). Ionospheric and thermospheric response to the 27-28 February 2014 geomagnetic storm over north Africa, Ann. Geophys., 36, 987–998. https://doi.org/10.5194/angeo-36-987-2018.

Manson, A. H., Meek, C. E., Gregory, J. B., (1981). Long-Period Oscillations in Mesospheric and Lower Thermospheric Winds (60-110km) at Saskatoon (52°N, 107°W, L=4.3). J. Geomag. Geoelectr., 33(12), 613-621.

Martinis, C., Meriwether, J., Niciejewski, R., Biondi, M., Fesen, C. and Mendillo, M. (2001). Zonal neutral winds at equatorial and low latitudes. Journal of Atmospheric and Solar-Terrestrial Physics. 63. 1559-1569. 10.1016/S1364-6826(01)00022-0.

Maute, A., M. E. Hagan, V. Yudin, H.-L. Liu, and E. Yizengaw (2015). Causes of the longitudinal differences in the equatorial vertical E×B drift during the 2013 SSW period as simulated by the TIME-GCM, J. Geophys. Res. Space Physics, 120, 5117–5136, doi:10.1002/2015JA021126.

Meriwether, J., Faivre, M., Fesen, C., Sherwood, P., and Veliz, O. (2008). New results on equatorial thermospheric winds and the midnight temperature maximum, Ann. Geophys., 26, 447–466, doi:10.5194/angeo-26-447-2008.

Meriwether, J. W., Makela, J. J., Huang, Y., Fisher, D. J., Buriti, R. A., Medeiros, A. F., and Takahashi, H. (2011). Climatology of the nighttime equatorial thermospheric winds and temperatures over Brazil near solar minimum, *J. Geophys. Res.*, 116, A04322, doi:10.1029/2011JA016477.

Pancheva, D., N. Mitchell, R. R. Clark, J. Drobjeva, and J. Lastovicka (2002). Variability in the maximum height of the ionospheric F2-layer over Millstone Hill (September 1998–March 2000); influence from below and above, Ann. Geophys., 20, 1807–1819, doi:10.5194/angeo-20-18072002.

Panda, D., Senapati, B., Tyagi, B., Kundu, B. (2018). Effects of Rayleigh-Taylor instability and Ionospheric plasma bubbles on the Global Navigation Satellite System signal. Journal of Asian Earth Sciences. 170. 10.1016/j.jseaes.2018.11.006.

Portnyagin, YI. and Solovjova, T. (1999). Global empirical wind model for the upper mesosphere/lower thermosphere. I. Prevailing wind. Annales Geophysicae. 18. 10.1007/s00585-000-0300-y.

Qian Wu, R. Daniel Gablehouse, Stanley C. Solomon, Timothy L. Killeen, Chiao-Yao She (2004). "A new Fabry-Perot interferometer for upper atmosphere research," Proc. SPIE 5660, Instruments, Science, and Methods for Geospace and Planetary Remote Sensing; doi: 10.1117/12.573084.

Rabiu, A. B., Yumoto, K., Falayi, E.O., Bello O. R, and MAGDAS/CPMN Group, (2011). Ionosphere over Africa: Results from Geomagnetic Field Measurements During International Heliophysical Year IHY. Sun and Geosphere, 6(2): 61-64.

Rabiu, A. B., Folarin, O. O., Uozumi, T., Abdul Hamid, N. S., and Yoshikawa, A., (2017). Longitudinal variation of equatorial electrojet and the occurrence of its counter electrojet, Ann. Geophys., 35, 535-545, doi:10.5194/angeo-35-535-2017.

Raghavarao, R., Suhasini, R., Hoegy, W.R., Mayr, H.G., Wharton, L. (1998). Local time variation of equatorial temperature and zonal wind anomaly. Journal of Atmospheric and Solar-Terrestrial Physics 60, 631– 642.

Reid, I., Spargo, A., Woithe, J., (2014). Seasonal variations of the night-time O (1S) and OH(8-3) airglow intensity at Adelaide, Australia. Journal of Geophysical Research: Atmospheres, 119(11), 6991-7013.

Richmond, A. D, Ridley E. C., Roble R. G. (1992). A thermosphere/ionosphere general circulation model with coupled electrodynamics. Geophys Res Lett 19:601-604.

Shiokawa K, Otsuka Y, Oyama S, Nozawa S, Satoh M, Katoh Y, Hamaguchi Y, Yamamoto Y, Meriwether J (2012). Development of lowcost sky-scanning Fabry–Perot interferometers for airglow and auroral studies. Earth Planets Space 64(11):1033–1046. https://doi.org/10.5047/eps.2012.05.004

Tesema, F., Mesquita, R., Meriwether, J., Damtie, B., Nigussie, M., Makela, J., Fisher, D., Harding, B., Yizengaw, E., and Sanders, S. (2017). New results on equatorial thermospheric winds and temperatures from Ethiopia, Africa, Ann. Geophys., 35, 333–344, https://doi.org/10.5194/angeo-35-333-2017.

Vila, P., Rees, D., Merrien, P. and Kone, E. (1998). Fabry-Perot interferometer measurements of neutral winds and F2 layer variations at the magnetic equator, Ann. Geophysicae 16, 731-737.

Wernik, A., Alfonsi, L., Materassi, M. (2004). Ionospheric irregularities, scintillation and its effect on systems. Acta Geophysica Polonica. 52.

Xu, J., R. Ma, and W. Wang (2012). Terannual variation in the F2 layer peak electron density (NmF2) at middle latitudes, J. Geophys. Res., 117, A01308, doi:10.1029/2011JA017191.

Xu, H., Shiokawa, K., Oyama, S, (2019). Thermospheric wind variations observed by a Fabry–Perot interferometer at Tromsø, Norway, at substorm onsets, Earth Planets Space 71, 93, https://doi.org/10.1186/s40623-019-1072-0.

583 Yiyi Huang, Jonathan J. Makela, and Gary R. (2012). Swenson Simulations of imaging
584 Fabry–Perot interferometers for measuring upper-atmospheric temperatures and winds.
585 Optical Society of America, 10 June 2012 / Vol. 51, No. 17 / APPLIED OPTICS.

586 Yizengaw, E., Moldwin, M. B., Zesta, C., Biouele, C. M., Damtie, B., Mebrahtu, A., Rabiu,
587 A. B., and Stoneback, R. (2014). The longitudinal variability of equatorial electrojet and
588 vertical drift velocity in the African and American sectors, Ann. Geophys., 32, 231–238,
589 www.ann-geophys.net/32/231/2014/, doi:10.5194/angeo32-231-2014.

590 Yoon, M., and J. Lee (2014). Medium scale traveling ionospheric disturbances in the
591 Korean region on 10 November 2004: Potential impact on GPS-based navigation systems,
592 Space Weather, 12, 173–186, doi:10.1002/2013SW001002.

593

594